J. Indian Inst Sci., Mar–Apr. 1996, **76**, 183–199.

Modelling of single-mode diffused channel optical waveguides

ANURAG SHARMA[1] AND PUSHPA BINDAL[2]
[1]Physics Department, Indian Institute of Technology, New Delhi 110 016, (email: asharma@physics.iitd.ernet.in)
[2]Kalindi College, Delhi University, New Delhi 110 008.

Received on November 2, 1994 ; Revised on August 14, 1995.

Abstract

We present some methods based on the variational principle for modelling of diffused channel waveguides and directional couplers. First, we present some analytical trial fields to model the mode of the channel waveguides. These are obviously limited in accuracy by the choice of the form of the trial field. To improve upon this aspect, we present a numerical method in which the trial field is automatically generated. This gives much better accuracy. Finally, we use these methods to model the characteristics of a directional coupler and compare the results with available experimental results.

Keywords: Optical waveguides, optical directional couplers, variational method, diffused channel waveguides.

1. Introduction

Diffused channel waveguides are basic elements in several integrated optical devices such as directional couplers, interference filters, optical switches, etc. These waveguides have two-dimensional graded refractive index profiles and the scalar wave equation does not have closed-form field solutions. Therefore, to study the propagation characteristics of such waveguides, one uses either direct numerical methods[1–3] or approximate methods[4–6]. The numerical methods based on finite-difference[1,2] or finite-element[3] methods involve extensive computations and do not lead to simple analytical forms for the modal fields. This has led to the development of a number of approximate methods[4–6] which are based on the variational principle. Accuracy of the methods based on variational principle depends on the closeness of the assumed trial field to the exact modal field of the guiding structure. The three approximate methods[4–6] basically differ only in the form of the trial modal field and in all these methods it has been assumed that the scalar modal field is separable in its dependence along the width and depth. We have recently developed a numerical method[7] which is based on the scalar variational principle and gives an optimal accuracy under the assumption of separable fields.

In this paper, we discuss some of the methods for the analysis of diffused channel waveguides that we have developed recently. These methods are based on the variational principle and, therefore, after discussing the general characteristics of wave propagation through channel waveguides in Section 2, we have included the basic features of the variational method in Section 3. In Section 4, we discuss the analytical approximations

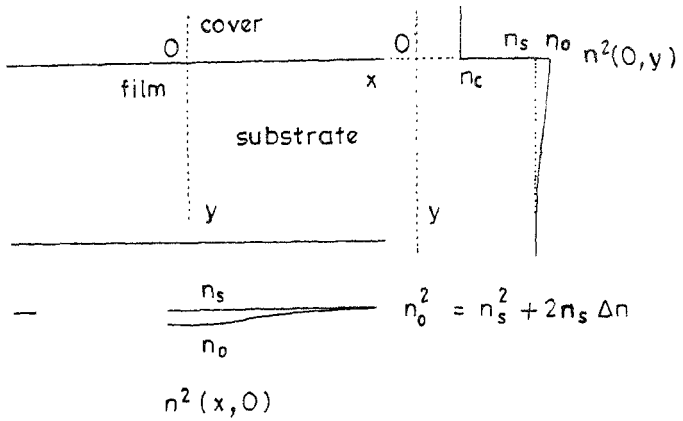

FIG. 1. *Schematic of the refractive index distribution in a diffused channel waveguide.*

for the modal field and Section 5 is devoted to the optimal variational numerical method. Finally, in Section 6, we apply these methods for obtaining characteristics for directional couplers consisting of diffused channel waveguides.

2. Modes of channel waveguides

To effectively analyse and design the channel waveguides, it is necessary to understand the phenomenon of guidance through them. In the most basic form, this requires the solutions of Maxwell's equations for the boundary conditions represented by the waveguiding structure. Fortunately, for optical waveguides, in most cases of practical importance, the conditions are such that the vector nature of optical waves can be ignored, at least to a very good approximation, and then, it suffices to solve the much simpler Helmholtz equation. This 'simpler' Helmholtz equation, however, is still difficult to solve for integrated optical structures such as diffused channel waveguides which provide two-dimensional confinement to optical waves. In this case, the Helmholtz equation is a partial differential equation and one has to use approximate and/or numerical techniques to obtain its solutions.

The refractive index profile of a channel optical waveguide can be represented as (see Fig. 1)

$$n^2(x,y) = \begin{cases} n_s^2 + 2n_s \Delta n\, f(x) g(y) & y > 0 \\ n_c^2 & y < 0 \end{cases} \tag{1}$$

where n_s is the refractive index of the substrate, n_c, the index of the cover (usually air) and Δn, the maximum index change from substrate to the guiding region. In fact, $n_0 = \sqrt{(n_s^2 + 2n_s\Delta n)} \approx n_s + \Delta n$ is the maximum index of the film, generally at the central point ($x = 0$) on the top surface ($y = 0$) of the waveguide film. The Helmholtz equation for such a guiding structure is given by

$$\frac{\partial^2\Psi}{\partial x^2} + \frac{\partial^2\Psi}{\partial y^2} + \frac{\partial^2\Psi}{\partial z^2} + k_0^2 n^2(x,y)\Psi(x,y,z) = 0 \tag{2}$$

where $\Psi(x,y,z)$ is one of the transverse Cartesian components of the electric field. The time dependence of the field is assumed to be of the form $\exp(i\omega t)$ and $k_0 = \omega/c$. Since the refractive index is independent of z, the z-dependence of Ψ can be separated out and a solution of eqn 2 can be assumed to be of the form

$$\Psi(x,y,z) = \psi(x,y)e^{-i\beta z} \tag{3}$$

where $\psi(x,y)$ satisfies the two-dimensional Helmholtz equation

$$\frac{\partial^2\psi}{\partial x^2} + \frac{\partial^2\psi}{\partial y^2} + \left[k_0^2 n^2(x,y) - \beta^2\right]\psi(x,y) = 0 \tag{4}$$

and β is a constant referred to as the propagation constant. Equation 4 is in fact an eigenvalue equation with β being the eigenvalue and $\psi(x, y)$ the eigenfunction of the operator $\partial^2/\partial x^2 + \partial^2/\partial y^2 + k_0^2 n^2(x, y)$. Thus, eqn 4 admits only certain discrete solutions, called the guided modes and a continuum of solutions called the radiation modes. It is the guided modes that represent the confinement of waves in the waveguide whereas the radiation modes are not 'bound' to the guiding region. The function $\psi(x, y)$ is the field pattern of the mode and β, the propagation constant of the mode, with ω/β being the phase velocity of the mode inside the waveguide along the z-axis. Depending on the value of Δn and the dimensions of the guiding region, and on the (vacuum) wavelength λ of the propagating wave, a waveguide may support a number of guided modes, each of which, in general, has a different β and $\psi(x, y)$. However, most important waveguides are the ones which allow only one guided mode—the so-called single-mode or monomode waveguides—since these are the basic elements of most integrated optical devices. We shall confine our discussion to such waveguides in this paper.

In a channel waveguide, the refractive-index distribution is symmetric along the surface of the waveguide (along the x-direction) and the commonly used functions to model the index variation are

$$f(x) = \begin{cases} \exp(-x^2/W^2) & \text{Gaussian} \\ \left[\operatorname{erf}\left\{\frac{x+W}{D}\right\} - \operatorname{erf}\left\{\frac{x-W}{D}\right\}\right]/[2\operatorname{erf}(W/D)] & \text{error function} \end{cases} \tag{5}$$

where W and D are constants related to the fabrication conditions. For example, in Ti-diffused $LiNbO_3$ waveguides, $2W$ is the width of Ti strip before diffusion and D, the

diffusion depth. The refractive-index distribution along the depth (the y-direction) is highly asymmetric and the commonly used functional forms for $g(y)$ are

$$g(y) = \begin{cases} \exp(-y/D) & \text{exponential} \\ \exp(-y^2/D^2) & \text{Gaussian} \\ \operatorname{erfc}(y/D) & \text{complementary error function.} \end{cases} \tag{6}$$

We have used these representations in our numerical examples for the normalized propagation constant, B, as a function of the normalized frequency, V, where

$$B = \frac{(\beta / k_0)^2 - n_s^2}{2 n_s \Delta n}, \qquad V = k_0 D \sqrt{2 n_s \Delta n}. \tag{7}$$

3. The variational principle

The variational principle which has been the basis of a number of methods used in the waveguide theory is based on the integral form of the Helmholtz equation. We have used this principle in developing our analytical models as well as the numerical method discussed in the present paper. Therefore, we briefly discuss here the salient features of this principle and its application to waveguide analysis.

The integral form of the Helmholtz equation (eqn 4) for a channel waveguide can be written as[8]

$$\beta^2 = \iint k_0^2 n^2(x,y) |\psi(x,y)|^2 \, dxdy - \iint |\nabla \psi|^2 \, dxdy \tag{8}$$

where both the integrals are over $-\infty$ to ∞ and it is assumed that the modal field is normalised

$$\iint |\psi(x,y)|^2 \, dxdy = 1. \tag{9}$$

The right-hand side (RHS) of eqn 8 is usually referred to as the stationary expression for the propagation constant, β, since it is stationary with respect to variations in $\psi(x,y)$. Since the modal field is an unknown function and, in fact, is the function that is sought for as the solution of the propagation problem, one uses an approximation for it as $\psi_t(x, y)$, generally referred to as the trial field. This trial field when used in eqn 8 gives an estimate of the propagation constant, say β_t. Thus, we have

$$\beta_t^2 = \iint k_0^2 n^2(x,y) \, |\psi_t(x,y)|^2 \, dxdy - \iint |\nabla \psi_t|^2 \, dxdy. \tag{10}$$

Different functions for $\psi_t(x, y)$ would give different values of β_t. An important property of this expression is that all these values of β_t would invariably be smaller than the exact value of β and the exact value is obtained *only* when $\psi_t(x, y)$ is the same as the exact modal field[8]. Thus, higher the value of β_t obtained using eqn 10, closer it is

to the exact value of β and better is the corresponding $\psi_t(x, y)$ as an approximation for the modal field. *Therefore, a value of β_t obtained through the variational expression necessarily represents a better approximation for β than any other approximation which has a smaller value.* This property is extremely useful in developing simple analytical models for the mode of a given waveguide, and the method employed is as follows:

A trial field $\psi_t(x, y; p_1, p_2, ..., p_n)$ is set up which involves a number of adjustable parameters $p_1, p_2, ..., p_n$. The dependence on x and y is chosen in such a way that ψ_t resembles the actual field as far as possible. This ψ_t is then substituted in the RHS of eqn 10 which is then maximized with respect to the parameters $p_1, p_2, ..., p_n$. The maximum value of β_t thus obtained is an estimate for the propagation constant and the corresponding $\psi_t(x, y; p_1, p_2, ..., p_n)$ with the optimized values of parameters $p_1, p_2, ..., p_n$ is an approximation for the modal field. Of various $\psi_t(x, y)$ obtained in this manner, the one which gives the largest value of β_t represents the best approximation for the modal field. Generally, by increasing the number of parameters, in a suitable fashion, one can generate better trial fields, but a better trial field with smaller number of parameters is always sought for, since it not only simplifies the computations, but also is easier to use for further modelling of devices involving these waveguides.

4. Analytical approximations for the modal fields

The Hermite–Gauss (HG) and the cosine-exponential (CE) trial fields have been developed and used mainly for channel waveguides; the former for diffused channel waveguides[5] and the latter for step-index channel waveguides[9–11]. The CE field has later[6] been used for diffused channel waveguides also. A common feature of these methods, in fact, of most approximate methods, is that the trial field $\psi_t(x, y)$ is approximated by a product of a function of x and a function of y, *i.e.*, $\psi_t(x, y)$ is assumed to be separable in x and y:

$$\psi_t(x, y) = \chi(x)\phi(y). \tag{11}$$

Various variational methods differ in their assumptions for the functional forms of $\chi(x)$ and $\phi(y)$. For the HG field, these are[5]

$$\chi_{HG}(x) \sim \exp(-x^2/\delta^2)$$

$$\phi_{HG}(y) \sim \begin{cases} (y/d)\ \exp(-y^2/d^2) & y \geq 0 \\ 0 & y \leq 0 \end{cases} \tag{12}$$

where δ and d are the variational parameters. The field in the cover region is again neglected. The CE field is given by[9–11]

$$\chi_{CE}(x) \sim \begin{cases} \cos(qx/W) & |x| \leq \eta W \\ \cos(q\eta)\exp[-q\tan(q\eta)(x/W - \eta)] & |x| \geq \eta W \end{cases}$$

$$\phi_{CE}(y) \sim \begin{cases} \cos(p\sigma)\exp[(p\tan p\sigma)(y/d)] & y \le 0 \\ \cos[p\{(y/d)-\sigma\}] & 0 \le y \le \xi d \\ \cos[p(\xi-\sigma)]\exp[-p\tan\{p(\xi-\sigma)\}(y/d-\xi)] & y \ge \xi d \end{cases} \quad (13)$$

where p, q, σ, ξ and η are the five variational parameters. CE results, though much better than the HG results when applied to planar and channel waveguides, still have considerable error in spite of the large number of parameters in the trial field. (The error is typically a few per cent in B).

We have presented recently[12] a better trial field using the secant hyperbolic (SH) functions:

$$\chi_{SH}(x) \sim \operatorname{sech}^{\rho}(x/W)$$

$$\psi_{SH}(y) \sim \begin{cases} \sinh(y/D)\operatorname{sech}^{\tau}(y/D) & y \ge 0 \\ 0 & y \le 0 \end{cases} \quad (14)$$

where ρ and τ are the variational parameters with field in the cover neglected. Along the depth (y-axis), both HG and SH fields are the first antisymmetric modes of specific profiles—the infinite parabolic and the sech^2, respectively, with the field for $y < 0$ suppressed, and along the surface (x-axis) these are the corresponding first symmetric modes. In both the HG and SH models, the field in the cover region ($y \le 0$) has been neglected. Although it is a fairly good approximation, it is the main cause of lower accuracy at lower V values. We have also developed[16] a simple method to improve the HG and SH fields on account of the field in the cover region. The improved field resembles the mode of the given profile remarkably well both in the guiding and cover regions. The explicit form of the improved HG—the evanescent Hermite–Gauss (EHG)—field is then given by[16]

$$\phi_{EHG}(y) \sim \begin{cases} (1+W_c y)\exp(-y^2/d^2) & y \ge 0 \\ \exp(W_c y) & y \le 0 \end{cases} \quad (15)$$

with

$$W_c = \sqrt{(\beta_t^2 - k_0^2 n_c^2)}. \quad (16)$$

The expression for the evanescent secant-hyperbolic (ESH) field is given by[12]

$$\phi_{ESH}(y) \sim \begin{cases} [1+W_c\sinh(y/D)]\ \operatorname{sech}^{\tau}(y/D) & y \ge 0 \\ \exp(W_c y) & y \le 0 \end{cases} \quad (17)$$

with

$$W_c = \sqrt{(\beta^2 - k_0^2 n_c^2)}. \quad (18)$$

The function $\chi(x)$ remains unchanged in the improved fields. The two variational parameters and β_t are obtained by maximizing the RHS of eqn 10 using the trial field

Table I
Results for channel waveguides
(Values of $B = \left[(\beta/k_0)^2 - n_f^2\right]/2n_s\Delta n$)

V	V_{OPT}	HG	EHG	SH	ESH	CE
2.12	0.133	0.112	0.125	0.118	0.130	0.123
2.59	0.248	0.233	0.247	0.231	0.245	0.234
3.00	0.329	0.313	0.328	0.313	0.327	0.318

$\chi(x)\phi(y)$. The field $\phi(y)$ is then replaced by the improved trial field obtained using the method described above. Thus, the EHG field is obtained by replacing $\phi_{HG}(y)$ in eqn 12 by $\phi_{EHG}(y)$ of eqn 15, and $\chi_{EHG}(x) = \chi_{HG}(x)$. Similarly, the ESH field is obtained by replacing $\phi_{SH}(y)$ in eqn 14 by $\phi_{ESH}(y)$ of eqn 17, and $\chi_{ESH}(x) = \chi_{SH}(x)$. We obtain $\psi_{ESH}(x, y)$ and $\psi_{EHG}(x, y)$ from $\psi_{SH}(x, y)$ and $\psi_{HG}(x, y)$, respectively, *without* the addition of any parameter and a *single* evaluation of the RHS of eqn 10 is required in each case for this improvement. An example of numerical values of B obtained using these trial fields is given in Table I. The index profile of the waveguide used is error function along the x-axis (see eqn 5) and Gaussian along the y-axis (see eqn 6) with $W = 3$ μm and $D = 3.35$ μm. There are no exact values available for channel waveguides. In Table I, V_{OPT} refers to a numerical variational method that we have developed and is described in Section 5. This method gives the *best* estimate for β under the assumption of separability (eqn 11). Since the value of B obtained using the V_{OPT} method is the largest, these are definitely closer to the exact values (which are still larger than, or equal to, V_{OPT} values) than the values of B obtained using other trial fields. Thus, the V_{OPT} values serve as the most accurate values for the present comparison. Table I shows that the CE method, which now has five parameters, is in considerable error, while the EHG and ESH are comparable.

5. The optimal numerical variational method

In the variational methods described above the accuracy is limited by the assumption of separability (eqn 11) and by the assumption of specific field forms for $\chi(x)$ and $\phi(y)$. We have developed a method[7,13] in which any specific form of $\chi(x)$ and $\phi(y)$ are not assumed and these are automatically generated by the variational method in the process of optimization. However, the separability is still assumed. Thus, under the assumption of separability, this method generates an *optimal* trial field and gives the *best* accuracy for the propagation constant. The numerical results discussed later in this section show this explicitly.

5.1. *Basic equations*

As mentioned above, we continue with the assumption of separability. Thus, with $\psi_t(x, y)$ substituted from eqn 11 into the variational expression, eqn 10 takes the form

$$\beta_t^2 = \iint k_0^2 n^2(x,y)|\chi(x)|^2\,|\phi(y)|^2\,dxdy - \int |d\chi/dx|^2\,dx - \int |d\phi/dy|^2\,dy \qquad (19)$$

where it is assumed that both $\chi(x)$ and $\phi(y)$ are normalised

$$\int |\chi|^2 dx = 1 = \int |\phi|^2 dy. \tag{20}$$

Our method is iterative and we assume, to start with, a planar index distribution $n_x^2(x)$ (it could as well be $n_y^2(y)$). We introduce this index distribution into the variational expression of eqn 19 which can be rewritten as[13]

$$\beta^2 = \int k_0^2 n_x^2(x)|\chi(x)|^2 dx - \int |d\chi/dx|^2 dx + \int k_0^2 |\phi(y)|^2 \left[\int \{n^2(x,y) - n_x^2(x)\} |\chi(x)|^2 dx \right] dy - \int |d\phi/dy|^2 dy. \tag{21}$$

Equations 19 and 21 are identical since the terms containing $n_x^2(x)$ cancel out exactly. However, in writing the equation in this manner, we have separated the RHS in two terms (written on two separate lines). We will show in the following that each of these terms is positive and can be uniquely maximized giving, thus, the maximum value of β_x.

The first term, $\int k_0^2 n_x^2 |\chi|^2 dx - \int |d\chi/dx|^2 dx$ is the variational expression for the planar index profile, $n_x^2(x)$, and hence is equal to the square of the propagation constant, say β_x^2, of its mode. It is thus positive and has a maximum value β_x^2. This value can be obtained exactly using a standard numerical method[14]. The function $\chi(x)$ is simply the corresponding modal field which can be normalised to satisfy the condition of eqn 20. We have thus obtained the maximum value of the first term of eqn 21 and have generated the function $\chi(x)$.

The second term of eqn 21 is also in the form of the variational expression for a planar index distribution, $n_y^2(y)$ which is defined as

$$n_y^2(y) = \int \{n^2(x,y) - n_x^2(x)\} |\chi(x)|^2 dx \tag{22}$$

which can be easily evaluated using $n_x^2(x)$ and $\chi(x)$ of the first term. Thus, the second term is also positive and its maximum value is β_y^2, where β_y is the propagation constant of the waveguide defined by $n_y^2(y)$ of eqn 22. The value of β_y and the corresponding modal field $\phi_y(y)$ can be easily obtained numerically. The field $\phi_y(y)$ can then be normalised as required by eqn 20.

Next, we use $n_y^2(y)$ generated above to rewrite the variational expression of eqn 19 as

$$\beta^2 = \int k_0^2 n_y^2(y)|\phi(y)|^2 dy - \int |d\phi/dy|^2 dy + \int k_0^2 |\chi(x)|^2 \left[\int \{n^2(x,y) - n_y^2(y)\} |\phi(y)|^2 dy \right] dx - \int |d\chi/dx|^2 dx. \tag{23}$$

The first term on the RHS of eqn 23 is exactly the same as the second term of eqn 21 and has already been maximized. The second term, in eqn 23, is again a variational expression for the index profile $n_x^2(x)$ which is now defined as

$$n_x^2(x) = \int \{n^2(x,y) - n_y^2(y)\} |\phi(y)|^2 \, dy \tag{24}$$

where $n_y^2(y)$ and $\phi(y)$ are obtained in the first term of eqn 23. The second term, thus, has a maximum value β_x^2 where β_x is the propagation constant of the mode of a waveguide with the profile $n_x^2(x)$, now defined by eqn 24.

This completes one cycle of iteration; starting from an arbitrary $n_y^2(x)$, we have generated a new $n_x^2(x)$ through the variational expression for the given index profile $n^2(x, y)$. This $n_x^2(x)$ is the starting point for the next cycle of iteration. The quantity $\beta_x^2 + \beta_y^2$ gives an estimate of the propagation constant β^2 of the mode of the given channel waveguide $n^2(x, y)$. At the end of each cycle of iteration, one checks for convergence in this quantity and the iterations are stopped when the convergence to a required accuracy is achieved. In most cases, one requires 2–3 iterations to obtain convergence to about 4 digits in B.

5.2. *Implementation procedure*

The method described above can be implemented as an iterative procedure for obtaining the propagation characteristics of a channel waveguide. Various steps required for this implementation are outlined below:

STEP 1 : Choose an $n_x^2(x)$. A good choice is $n_x^2(x) = n^2(x, y = 0)$.

STEP 2 : Obtain β_x^2 and $\chi(x)$ numerically. Normalize $\chi(x)$.

STEP 3 : Obtain $n_y^2(y)$ using eqn 22.

STEP 4 : Obtain β_y^2 and $\phi(y)$ numerically for $n_y^2(y)$. Normalize $\phi(y)$.

STEP 5 : Obtain $n_x^2(x)$ using eqn 24.

STEP 6 : Obtain β_x^2 and $\chi(x)$ numerically for $n_x^2(x)$. Normalize $\chi(x)$.

STEP 7 : Compute $\beta_t^2 = \beta_x^2 + \beta_y^2$. Check for convergence in β_t^2.
If converged, GOTO STEP 8
otherwise, GOTO STEP 3

STEP 8 : β_t^2 and $\psi_t(x, y) = \chi(x)\phi(y)$ are the required propagation constant and modal field.

For translation of this procedure into a computer program, one requires the following three elements:

1. Computation of the propagation constant of a planar waveguide. We have used the Ricatti transformation[14] and have solved the resulting first-order differential equation using the predictor–corrector method[15].

2. Computation of the modal field. We have used the predictor–corrector method for the Helmholtz equation directly.

3. Integration over the field to normalize it and to obtain the index distribution in the orthogonal direction (eqns 22 or 24). We have used Bode's 4-point formula[15] for evaluation of integrals, since the truncation error of this formula is of the same order as that of the predictor–corrector method.

Other details for implementation are given elsewhere[7].

5.3. *Numerical results and comparisons*

We discuss in this section some specific numerical examples to show the accuracies of various methods discussed above in comparison to other available methods. In particular, we will include the following methods in our comparisons:

1. VFD: Scalar finite-difference method based on the variational principle. Numerical results[2] have been obtained using a 14×14 mesh point grid in the transverse cross-section.
2. HFD: A direct vector finite-difference method[1] based on the magnetic (H) field components with typically 20×20 mesh point grid in the trans verse cross-section.
3. HG : The Hermite–Gauss (HG) method of Korotky *et al.*[5]

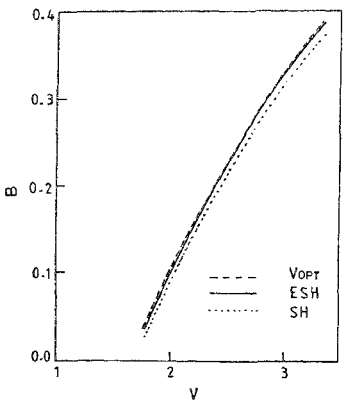

FIG. 2. Normalized propagation constant, B, as a function of the normalized frequency, V, for a diffused channel waveguide with an error function–Gaussian profile with parameters: $n_s = 2.203$, $n_c = 1.0$, $\lambda = 1.3$ μm, $D = 3.35$ μm and $W = 3.0$ μm.

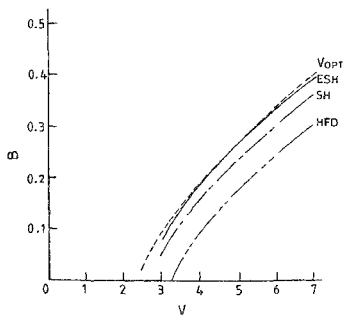

FIG. 3. Normalized propagation constant, B, as a function of V for a diffused channel waveguide with Gaussian-exponential profile with parameters: $n_s^2 = 2.0$, $n_c = 1.0$, $\lambda = 1.3$ μm, $D/W = 1$ and $n_0 = 1.05\, n_s$.

4. EHG : Variational method with evanescent Hermite–Gauss (EHG) trial field[16].

5. SH & ESH : Variational method with secant hyperbolic (SH) and evanescent secant hyperbolic (ESH) trial fields[12]

6. V_{OPT} : The optimal variational method discussed above. Typically 200 points are used for each one-dimensional analysis, and three or less iterations are required[7] for each V value.

The first numerical example is for an error function–Gaussian profile (error function in x-direction and Gaussian in y-direction). This profile has been studied by Korotky *et al.*[5] Figure 2 incorporates the results of SH, ESH and V_{OPT} methods, and shows that the results of ESH are nearly coincident with the results of V_{OPT} for the range of V values which are important for single mode operation. This shows that the ESH field is an extremely good approximation for mode of such a waveguide. The next example is a Gaussian exponential profile which has been studied by Schulz *et al.*[1] using HFD method. The results of HFD and also of ESH methods are given in Fig. 3. This figure shows that the results of HFD are grossly inaccurate while those of ESH are once again extremely close to V_{OPT} results which are close to the exact results as they represent the largest values of β. Another comparison with finite-difference method is shown in Fig. 4 in which the results of a Gaussian–Gaussian profile are given. The figure includes results obtained using V_{OPT}, ESH, HFD and VFD methods. This figure also shows that the finite-difference methods (both HFD and VFD) give very poor accuracy whereas ESH continues to be extremely accurate and almost coincident with V_{OPT} results except for very small V values. The low accuracy of VFD and HFD results can be ascribed to rather small size, 14×14 and 20×20, respectively, of the grid for sampling the field in the transverse cross-section. In the case of V_{OPT}, in which one has to consider only an one-dimensional sampling of the field at a time, the field is sampled, in effect, on a grid of size 200×200. In addition, in the finite-difference methods, one assumes that the field vanishes at the boundaries of a window whose size is kept large enough to keep the effect of this approximation at a negligible level. However, the larger the size of the win-

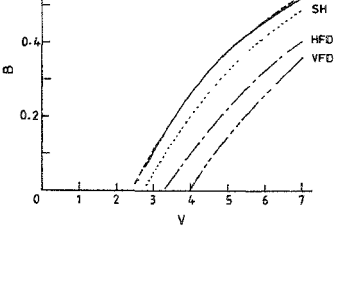

FIG. 4. Normalized propagation constant, B, as a function of V for a diffused channel waveguide with Gaussian–Gaussian profile with parameters: $n_s^2 = 2.1$, $n_c = 1.0$, $\lambda = 1.3$ μm, $D/W = 1$ and $n_0 = 1.05$ n_s.

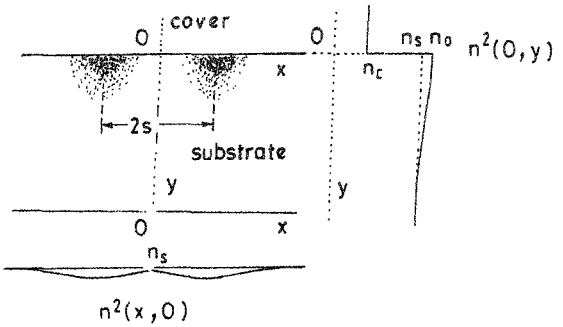

FIG. 5. Schematic of the index profile of a directional coupler made of two parallel diffused channel waveguides.

dow, more are the grid points required to sample the field so that these are close enough to approximate its variation adequately. On the other hand, in V_{OPT}, the field is assumed to decay exponentially outside the computational grid. These two aspects of finite-difference (and also finite-element) methods limit the accuracy rather severely unless very large computer memory and time are at disposal. The grid sizes of 20×20, used in HFD and 14×14, used in VFD, are highly inadequate as shown by the above results.

6. Directional couplers

Directional couplers are the basis for a variety of integrated optical devices such as switches, modulators, and power dividers. A directional coupler consists of two identical waveguides placed parallel to each other along the z-axis separated by a constant distance (see Fig. 5). (In some special applications, the waveguides may be non-identical and/or the separation between them may not be constant). The modes of the two waveguides, due to the overlap of their evanescent fields, get coupled to each other and exchange power between them as they propagate along the z-axis. Diffused waveguide directional couplers have been widely studied, both experimentally[17–19] and theoretically[4,18,20–24].

The refractive index profile for a directional coupler made up of two diffused channel waveguides can be written as (Fig. 5)

$$n^2(x,y) = \begin{cases} n_s^2 + 2n_s\Delta\tilde{n}g(y)[f(x-s)+f(x+s)] & y>0 \\ n_c^2 & y<0 \end{cases} \tag{25}$$

where $2s$ is the separation between the centres of the two constituent channel waveguides. The composite waveguiding structure thus formed has two modes, one of

which is symmetric and the other antisymmetric. The propagation constant of these modes, β_s and β_a, respectively, depends on the separation parameter, s, and is such that $\beta_s \geq \beta \geq \beta_a$ (β being the propagation constant of the isolated waveguide). The equality holds when the waveguides are widely separated (large values of s) so that their evanescent fields (along x) are vanishingly small and there is no interaction between them. In this limit, β_s, $\beta_a \to \beta$. Due to different propagation constants, the modes propagate with different phase velocities and hence acquire phase at different rates as they propagate along the length of the directional coupler, the z-axis. This leads to a z-dependent phase difference between them which shows up as intensity variation along the z-axis (since they have different field distributions). The effect of this characteristics is that when light is launched in one of the waveguides, say the one centred at $x = -s$, the two modes of the directional coupler are simultaneously excited, say in phase. After propagating through a certain distance, the modes will be exactly out of phase and the intensity will be maximum in the other waveguide (centred at $x = s$). Thus, in effect, the power has transferred from one waveguide to the other. This distance, after which the maximum power is transferred from one waveguide to the other, is called the coupling length, l_c, and is defined as

$$l_c = \frac{\pi}{\beta_s - \beta_a}. \tag{26}$$

This coupling length is the main parameter of a directional coupler and different methods have been used to obtain its value from the given refractive index profile. We discuss here the application of the V_{OPT} and ESH methods for obtaining the coupling length of diffused channel directional couplers.

6.1. *The V_{OPT} method*

As mentioned above, to obtain the coupling length, l_c, of a directional coupler, one has to obtain the propagation constants of the first symmetric and the first antisymmetric modes, β_s and β_a, respectively. In the two-dimensional numerical method[25], the composite waveguiding structure, defined by eqn 25, is considered to be one waveguide and its first two modes are obtained, individually, using the numerical method V_{OPT} (described in Section 5). The coupling length of the coupler (eqn 26) is then computed using the propagation constants of these modes.

6.2. *The ESH method*

In Section 4, we have discussed the evanescent secant-hyperbolic (ESH) trial field for the analysis of channel waveguides. We now extend the same method to obtain the coupling length of directional couplers made of two such waveguides. Various steps of analysis are summarized below:

- Use the secant hyperbolic (SH) trial field (eqn 14) for a single constituent waveguide to obtain ρ and τ.
- Modify $\phi(y)$ to include the field in the cover (*i.e.*, derive an ESH field; eqn 17).

- Use $\chi_{SH}(x)$ to construct the symmetric and the antisymmetric fields:

$$\chi_s(x) \sim \operatorname{sech}^p[(x-s)/W] + \operatorname{sech}^p[(x+s)/W] \tag{27}$$

$$\chi_a(x) \sim \operatorname{sech}^p[(x-s)/W] - \operatorname{sech}^p[(x+s)/W] \tag{28}$$

- Using $\chi_s(x)\phi_{ESH}(y)$ and $\chi_a(x)\phi_{ESH}(y)$ in variational expression (eqn 10), one obtains β_s and β_a, respectively, *without* any maximization.
- Obtain coupling length, l_t, using these β_s and β_a in eqn 26.

In this way, coupling length can be obtained without any maximization. This analysis is fairly accurate for relatively large values of s; however, for small values, when the waveguide modes influence each other rather strongly, a modification is necessary. In such cases, the peaks of the modes are no longer at the points where the index has the largest value. In fact, the peaks of the symmetric modes come closer to each other while those of antisymmetric modes become farther apart. This possibility is not taken into consideration in eqns 27 and 28. To take this aspect into account, we can modify the modes for the asymmetric and the antisymmetric mode by introducing a parameter, σ, such that

$$\chi_s(x;\sigma) \sim \operatorname{sech}^p[(x-\sigma)/W] + \operatorname{sech}^p[(x+\sigma)/W] \tag{29}$$

$$\chi_a(x;\sigma) \sim \operatorname{sech}^p[(x-\sigma)/W] - \operatorname{sech}^p[(x+\sigma)/W]. \tag{30}$$

The values of σ are such that $\sigma \leq s$ for the symmetric mode and $\sigma \geq s$ for the antisymmetric mode, and $\sigma \geq s$ for both modes for $s >> W$. The parameter σ is treated as a variational parameter for maximizing the variational expression (eqn 10) for the trial fields $\chi_s(x;\sigma)\phi_{ESH}(y)$ and $\chi_a(x;\sigma)\phi_{ESH}(y)$ to obtain β_s and β_a. These values of propagation constant then give improved value of the coupling length, l_c.

6.3. *Numerical results and comparison*

We now present an example to show the accuracy of the methods discussed above for directional couplers. We consider the directional couplers fabricated by Noda *et al.*[18] The profile assumed is Gaussian–Gaussian (see eqns 5 and 6) with parameters $n_s = 2.152$, $n_c = 1.0$, $\lambda = 1.153$ μm, $W = 4.0$ μm and $D = 5.0$ μm (Fig. 6). Two cases with $\Delta n = 0.004$ and $\Delta n = 0.006$ are included. Experimental results of Noda *et al.*[18] and the theoretical results using V_{OPT} and ESH are included in the figure. This figure shows that the results obtained using V_{OPT} and ESH methods are in very good agreement with the experimental data. This again brings out the point that V_{OPT} and ESH methods are extremely good methods for modelling and analysis of channel waveguides and devices made with these waveguides.

7. Conclusions

We have presented in this paper analytical and numerical methods based on variational principle for the analysis of diffused channel waveguides and directional couplers. In

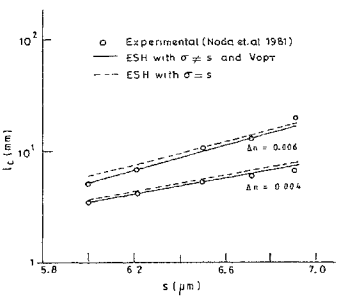

FIG. 6. Coupling length, L_c, as a function of s, one half of the waveguide separation for a directional coupler reported by Noda *et al.*[18]

particular, we have presented a trial field, the secant-hyperbolic field, which is much more accurate than the HG field while it retains the simplicity of the HG field. The improved version of this field, the evanescent secant-hyperbolic field, is extremely accurate and compares well with numerical methods which require much more computational effort.

We have also presented a numerical method (V_{OPT}) which gives the best accuracy in the propagation constant under the assumption that the trial field can be separated in its functional dependence on the width and the depth coordinates. This assumption, our results show, holds good for diffused channel waveguides. The numerical results show that, at least for the cases that we have discussed, the finite-difference (FD) methods give extremely poor accuracies in comparison to our method. In fact, even simple approximations such as the HG and SH trial fields are better than the FD methods. This could be due to rather small number of field sample points taken in these methods. The computational effort in an FD method is orders of magnitude higher than in the methods that we have described.

We have also included analysis of diffused channel waveguide directional couplers mainly to illustrate an application of the methods that we have developed. Comparisons with experimental data again show that the ESH method and the numerical method (V_{OPT}) perform extremely well in predicting the coupling length of directional couplers.

Acknowledgements

This work was partially supported by a grant from the National Institute for Standards and Technology (NIST, USA) and the Department of Science and Technology (DST, India).

References

1. SCHULZ, N., BIERWIRTH, K., ARNDT, F. AND KOSTER, U. Finite difference method without spurious solutions for the hybrid-mode analysis of diffused channel waveguides, *IEEE Trans.*, 1990, **MTT-38**, 722–729.

2. LAGU, R. K. AND RAMASWAMY, R. V — A variational finite difference method for analysing channel waveguides with arbitrary index profiles, *IEEE J.*, 1986, **QE-22**, 968–976.

3 YEH, C., HA, K., DONG, S. B. AND BROWN, W. P. — Single-mode optical waveguides, *Appl. Opt.*, 1979, **18**, 1490–1502

4 JAIN, U , SHARMA, A., THYAGARAJAN, K. AND GHATAK, A. K. — Coupling characteristics of a diffused channel waveguide directional coupler, *J. Opt. Soc. Am.*, 1982, **72**, 1545–1549

5. KOROTKY, S. K. *et al.* — Mode size and method for estimating the propagation constant of single mode Ti:$LiNbO_3$ strip waveguides, *IEEE J.*, 1982, **QE-18**, 1796–1802.

6. MISHRA, P. K. AND SHARMA, A. — Analysis of diffused channel waveguides, 18*th Opt. Soc of India Symp.*, Bangalore, India March 21–23, 1990.

7. SHARMA, A. AND BINDAL, P — An accurate variational analysis of single mode diffused channel waveguides, *Opt. Quantum Electron.*, 1992, **24**, 1359–1371

8. KOGELNIK, H. — Theory of optical waveguides. In *Integrated optics* (Tamir, T , ed.), 1975, p. 44, Springer Verlag.

9 SHARMA, A., MISHRA, P. K. AND GHATAK, A. K. — Analysis of single mode waveguides and directional couplers with rectangular cross section, *Proc. 2nd Eur. Conf. on Integrated Optics*, Florence, Italy, October 17–18, 1983, pp 9–12.

10 MISHRA, P. K., SHARMA, A., LABROO, S AND GHATAK, A. K. — Scalar variational analysis of single-mode waveguides with rectangular cross-section, *IEEE Trans.*, 1982, **MTT-33**, 282–286

11 SHARMA, A., MISHRA, P K. AND GHATAK, A. K. — Single-mode optical waveguides and directional couplers with rectangular cross section. a simple and accurate method of analysis, *J. Lightwave Technol.*, 1988, **6**, 1119–1125.

12 SHARMA, A. AND BINDAL, P. — Variational analysis of diffused planar and channel waveguides and directional couplers, *J. Opt. Soc. Am. A*, 1994, **11**, 2244–2248.

13. SHARMA, A. — On approximate theories of single mode rectangular waveguides, *Opt. Quantum Electron.*, 1989, **21**, 517–520

14. MISHRA, P. K. AND SHARMA, A. — Analysis of single mode inhomogenous planar waveguides, *J. Lightwave Technol.*, 1986, **LT-4**, 204–212.

15 ABRAMOWITZ, M. AND STEGUN, I. A — *Handbook of mathematical functions*, 1970, Dover.

16. SHARMA, A. AND BINDAL, P. — Analysis of diffused planar and channel waveguide, *IEEE J. Quantum Electron.*, 1993, **29**, 150–153.

17. ALFERNESS, R. C., SCHMIDT, R. V. AND TURNER, E. H. — Characteristics of Ti-diffused lithium niobate optical directional couplers, *Appl. Opt.*, 1979, **18**, 4012–4015.

18. NODA, J., FUKUMA, M. AND MIKAMI, O. — Design calculations for directional couplers fabricated by Ti-diffused $LiNbO_3$ waveguides, *Appl. Opt.*, 1981, **20**, 2284–2291.

19. KOROTKY, S. K. AND ALFERNESS, R. C. — The Ti:$LiNbO_3$ integrated-optic technology: fundamentals, design considerations and capabilities. In *Integrated optical circuits and components* (Hutcheson, L. D., ed.), 1987, Marcel Dekker.

20. SHARMA, A., SHARMA, E., GOYAL, I. C. AND GHATAK, A. K. — Variational analysis of directional couplers with graded-index profile, *Opt. Commun.*, 1980, **34**, 39–42.

21. PIET, M. D. AND FLECK, J. A. JR. — Comparison of calculated and measured performance of diffused channel-waveguide couplers, *J. Opt. Soc. Am.*, 1983, **73**, 1296–1310.

22. CTYROKY, J., HOFMAN, H., JANTA, J. AND SCHROFEL, J. 3-D analysis of $LiNbO_3$:Ti channel waveguides and directional couplers, *IEEE J.*, 1984, **QE-20**, 400–408.

23. KIM, C. M. AND RAMASWAMY, R. V. WKB analysis of asymmetric directional couplers and its application to optical switches, *J. Lightwave Technol.*, 1988, **6**, 1109–1118.

24. HAWKINS, R. T. II AND GOLL, J. H. Method for calculating coupling length of Ti:$LiNbO_3$ waveguide directional couplers, *J. Lightwave Technol.*, 1988, **6**, 887–891.

25. BINDAL, P. AND SHARMA, A. Modelling of Ti:$LiNbO_3$ directional couplers, *IEEE Photon. Technol. Lett.*, 1993, **4**, 729–731.